
Research Article

Effects of Molecular Weight and Loading on Matrix Metalloproteinase-2 Mediated Release from Poly(Ethylene Glycol) Diacrylate Hydrogels

Amy E. Ross,¹ Mary Y. Tang,² and Richard A. Gemeinhart^{1,2,3,4,5}

Received 17 January 2012; accepted 28 March 2012; published online 26 April 2012

Abstract. Herein, we report on continued efforts to understand an implantable poly(ethylene glycol) diacrylate (PEGDA) hydrogel drug delivery system that responds to extracellular enzymes, in particular matrix metalloproteinase-2 (MMP-2) to provide controlled drug delivery. By attaching peptide as pendant groups on the hydrogel backbone, drug release occurs at an accelerated rate in the presence of active protease. We investigated MMP-2 entry and optimized parameters of the drug delivery system. Mesh size for different PEGDA molecular weight macromers was measured with PEGDA 3,400 hydrogels having a mesh size smaller than the dimensions of MMP-2 and PEGDA 10,000 and PEGDA 20,000 hydrogels having mesh sizes larger than MMP-2. Purified MMP-2 increased release of peptide fragment compared to buffer at several loading concentrations. Cell-stimulated release was demonstrated using U-87 MG cells embedded in collagen. GM6001, an MMP inhibitor, diminished release and altered the identity of the released peptide fragment. The increase in ratio of release from PEGDA 10,000 and PEGDA 20,000 hydrogels compared to PEGDA 3,400 hydrogels suggests MMP-2 enters the hydrogel. PEGDA molecular weight of 10,000 and 15 % (w/v) were the optimal conditions for release and handling. The use of protease-triggered drug delivery has great advantage particularly with the control of protease penetration as a parameter for controlling rate of release.

KEY WORDS: cancer; chemotherapy; controlled drug delivery; enzyme-triggered drug delivery; matrix metalloproteinase-2; poly(ethylene glycol) diacrylate, hydrogel.

INTRODUCTION

Brain tumors are an uncommon but serious medical condition (1). It is estimated there will be 23,000 cases diagnosed and 13,000 deaths in the USA in 2011 (2). The most common primary brain malignancy is glioblastoma multiforme (GBM) (2). GBM is a swift killer, with a median survival time of 12 to 15 months and a 5-year survival rate of 3.4 % (3,4). New treatments are desperately needed since there are only few new treatments for this type of cancer in the last few decades. We report on the continued development (5–7) of an implantable hydrogel-based chemotherapy system with triggered release by the invasive nature of GBM and other cancers hoping that this will lead to new and improved treatments for this and other cancers.

Hydrogels are three-dimensional cross-linked polymers that are capable of absorbing large amounts of water (8). Hydrogels are well suited to drug delivery, as the high water content present in hydrogels while swollen and mechanics

make them similar to natural extracellular matrix and highly biocompatible (9). Hydrogels typically show little protein adsorption due to the low interfacial tension between the polymer matrix and surrounding aqueous solution (10). These properties are particularly important if the release mechanism being explored, *i.e.*, small molecule release attached through protease degradable pendant peptide, is similar to those that take place in natural extracellular matrix as a result of matrix metalloproteinase (MMP) degradation, *e.g.*, soluble extracellular bound proteins and extracellular matrix fragments (11).

MMPs are a family of over 20 zinc-dependent endopeptidases that are best known for degrading the extracellular matrix (12–14). MMP-2 is the most widely distributed MMP type throughout the body and is expressed by many cells (15,16). MMPs are expressed in a latent form and require activation in order to exhibit activity by the removal of the N-terminal propeptide domain (17). MMP levels have been demonstrated to be elevated in many forms of cancer (12). Members of the MMP family have been shown to be involved in various functions related to cancer such as tumor growth, cell migration, and tumor angiogenesis (18). MMP-2 has been increased in both expression and activation in glioblastomas compared to normal brain tissue (19,20). Overactive MMP-2 is a target for therapy and drug delivery for the treatment of malignancies (14). Peptide-drug conjugates, in which the drug is released or activated upon cleavage by MMP-2, have been successfully demonstrated *in vitro* and *in vivo* by several research groups (21–24). Micelles and other nanoparticles

¹ Department of Bioengineering, University of Illinois, Chicago, Illinois 60607-7052, USA.

² Department of Biopharmaceutical Sciences, University of Illinois, Chicago, Illinois 60612-7231, USA.

³ Department of Ophthalmology and Visual Science, University of Illinois, Chicago, Illinois 60612-4319, USA.

⁴ 833 South Wood Street (MC 865), Chicago, Illinois 60612, USA.

⁵ To whom correspondence should be addressed.(e-mail: rag@uic.edu)

using MMP-2-triggered release have also been utilized to exploit the enhanced permeation and retention effect in targeting solid tumors (25–28). Our group (5–7) and several others (29–37) have also applied this natural mechanism for drug release to hydrogel-based drug delivery systems for cancer and other diseases.

Using an MMP-2-triggered hydrogel-based drug delivery system for interstitial chemotherapy enables the drug to be released in the presence of elevated active MMP-2 and presumably, cancer cells. This drug delivery system uses poly (ethylene glycol) diacrylate (PEGDA). PEGDA is generally regarded as biocompatible and has been used in many drug delivery applications (10,38,39) and previously been approved for use by the FDA. Although generally regarded as poorly degrading or non-degrading, implantation of PEGDA hydrogels has resulted in significant degradation on the order of months (40). In this system, the drug, or model fluorescent dye, is conjugated to the hydrogel matrix *via* MMP-2 sensitive peptides. The sulfhydryl side chain on the cysteine is conjugated to a PEGDA acrylate group *via* Michael addition prior to cross-linking (41). Our previous work has shown that this drug delivery system released higher amounts of cisplatin when incubated with MMP-2 and showed greater toxicity to U-87 MG cells (5–7), but there was minimal specificity of release. Higher PEGDA macromer molecular weight (4 and 8 kg/mol) was associated with greater cisplatin release. To obtain maximum clinical effectiveness, the ideal PEGDA composition, PEGDA molecular weight, and drug loading must be determined. The optimum conditions maximize MMP-2 mediated release while minimizing nonspecific release and will allow MMP-2 to enter the hydrogel.

MATERIALS AND METHODS

All materials were purchased as chemical grade and used without further purification unless otherwise noted.

Hydrogel Creation

The fluorophore, tetramethyl rhodamine (TAMRA), was conjugated to the amino-terminal of the peptide sequence GPLGVRGC (UIC Protein Research Laboratory) using solid-phase synthesis and dissolved in double deionized water (DDIW) with PEGDA (Laysan Bio, Arab, AL) and stirred overnight. Hydrogels were polymerized by adding 35 μ L 20 % ammonium persulfate and 45 μ L of 20 % N-N'-N'-N'-tetramethylenediamine to the PEGDA solution. The precursor solution was fed into a mold consisting of two glass slides on either side of a 1/16" silicone rubber spacer (McMaster Carr, Elmhurst, IL). The mold was incubated for 30 min at 37 °C.

Mesh Size

Immediately after polymerization, hydrogel sheets were cut into 8-mm disks using a biopsy punch. Three disks were weighed while suspended in 1-butanol. Using Archimedes' principle, the volume was calculated by dividing the apparent weight by the density of butanol (42). The hydrogels were swollen in DDIW and re-weighed the next day in air. The hydrogels were weighed again in air at an interval of at least 3 h until equilibrium swelling was reached, defined by less than 5 % change in mass from the previous weighing. At that

point, the hydrogels were weighed again in butanol using the same procedure. The hydrogels were then freeze-dried using a Labonco lyophilizer for a minimum of 8 h. The xerogels were weighed in air. Mesh size was calculated (9,43) using equations based upon the Flory–Rehner swelling theory.

Release in the Presence of Active MMP-2

Immediately after polymerization, hydrogels were washed in tris buffered saline with zinc (TBS/Zn) to remove unconjugated peptide, unreacted macromer, and initiators. The buffer was composed of 50 mM tris base, 200 mM sodium chloride (NaCl), 10 mM calcium chloride dihydrate ($\text{CaCl}_2 \cdot 2\text{H}_2\text{O}$), 0.5 % Brij-35, and 50 μ M zinc sulfate heptahydrate ($\text{ZnSO}_4 \cdot 7\text{H}_2\text{O}$) and adjusted to pH 7.4. Washing continued until buffer fluorescence was stable between washes. Following this washing process, hydrogel disks with or without conjugated peptide were cut using a biopsy punch and incubated in a 96-well plate with either TBS/Zn or TBS/Zn with 9 nM active MMP-2 (EMD/Calbiochem, Gibbstown, NJ) at 37 °C. At each time point, the buffer fluorescence was measured with a Spectramax GeminiXS fluorescence plate spectrofluorometer (Molecular Devices Corporation, Sunnyvale, CA) at an excitation wavelength of 540 nm and an emission wavelength of 570-nm emission. Fluorescent values were compared to a standard curve of the cleaved peptide fragment. The remaining buffer was removed from the wells and replaced with MMP-2 resupplemented in appropriate groups.

Total peptide release from within hydrogels was determined by hydrolyzing hydrogels not used in the release experiment with 1N sodium hydroxide. Peptide within the hydrolyzed hydrogel solution was determined and compared to a standard curve from free peptide in 1N sodium hydroxide. The ratio of specific release (p_r) was calculated by dividing the peptide released in the presence of MMP-2 by the peptide released absence of MMP-2 at 96 h.

Release in the Presence of U-87 MG Cells

The human U-87 MG glioblastoma cell line (ATCC, Manassas, VA) was maintained in Eagle's minimum essential medium (Mediatech, Manassas, VA) supplemented with 10 % fetal bovine serum (Gemini), 1 % penicillin/streptomycin (Mediatech), 200 mM L-glutamine, and 110 mg/mL sodium pyruvate. Cells (1.0×10^6 cells/mL) were entrapped in collagen gels composed of 2.5 mg/mL collagen I (BD Biosciences, Franklin Lakes, NJ) by mixing a cell suspension with a collagen solution and incubating. Collagen gels without cells were made in the same manner with Dulbecco's phosphate buffered saline replacing the cell suspension. The collagen gels were incubated at 37 °C for 30 min to allow gelation. Gels were removed from the incubator and a total of 50 μ L serum-free Eagle's minimum essential medium, with or without 2.5 mM GM6001 was added and incubated for 2 h at 37 °C at which point stable collagen gels were observed.

Hydrogel rods were formed by polymerizing the monomer solution (as previously described) within polymer tubes of known diameter. Following polymerization, the rods were de-molded and rinsed in buffer as previously described. After rinsing, a specified length, 2.5 mm, of the rod was cut and inserted into a syringe needle. Using the syringe needle, the hydrogel rod was injected into the collagen gels. Samples

were collected by removing the hydrogel and centrifuging the remaining solution. The supernatant was filtered through a 0.45 μm syringe filter (Millipore, Billerica, MA) and stored at $-20\text{ }^{\circ}\text{C}$.

Supernatant was analyzed using a Symmetry C18 high-performance light chromatography (HPLC) column with a gradient mobile phase of acetonitrile (ACN) and filtered DDIW at a rate of 1 mL/min for 60 min. The initial mobile phase composition was 20 % ACN/80 % DDIW and the final concentration was 80 % ACN/20 % DDIW. Samples were detected using a Waters fluorescence detector set to 540 nm excitation, 570-nm emission wavelengths (Waters Corporation, Milford, MA).

Cleaved Product Identification

Fractionated peaks from HPLC were analyzed using matrix-assisted laser desorption ionization/time-of-flight (MALDI/TOF) mass spectrometry. Samples (1 μL) were mixed with 1 μL of saturated matrix solution (*a*-cyano-4-hydroxycinnamic acid in 1:1 acetonitrile and water). Matrix-sample mixture (1 μL) was spotted onto a MALDI plate and analyzed using a Voyager-DE PRO high-performance bench-top MALDI-TOF mass spectrometer (Applied Biosystems, Foster City, CA, USA) equipped with a 337-nm pulsed nitrogen laser. Mass spectra were acquired in a linear positive mode.

Gelatin Zymography

Gelatin zymography was performed on conditioned media from the U-87 MG cells embedded in collagen using a MiniPROTEAN II electrophoresis cell and Ready Gel® Zymogram Gels (Bio-Rad, Hercules, CA). Samples were diluted 1:2 in a sample buffer consisting of 62.5 mM Tris-HCl, 4 % sodium dodecyl sulfate (SDS), 25 % glycerol, and 0.01 % bromophenol blue. Active MMP-2 was used as a control in 0.5 M Tris-HCl at a concentration of 9 nM. The gel was run in a buffer consisting of 25 mM tris, 192 mM glycine, and 0.1 % SDS. The gel was run at a voltage of 100 V for 60–70 min. The gel was renatured in a solution of 2.5 % Triton X-100 for 30 min. The gel was then washed in a development solution of 50 mM tris base, 200 mM NaCl, 5 mM $\text{CaCl}_2\cdot 5\text{H}_2\text{O}$, and 0.02 % Brij-35 for 5 min and incubated in development solution overnight. The gel was stained with a solution of 10 % acetic acid, 40 % methanol, 50 % DDIW, and 0.5 % R-250 Brilliant Blue (Coomassie) for 1 h. The gel was destained with a solution of 10 % acetic acid, 40 % methanol and 50 % DDIW until the stacking portion was clear, changing the destaining solution as needed.

Table I. Acrylate Group Concentration in PEGDA Hydrogel Compositions

PEGDA molecular weight (g/mol)	Acrylate concentration (mM)		
	10 %	15 %	20 %
Composition (w/V %)			
3,400	59	88	118
10,000	20	30	40
20,000	10	15	20

Statistics

All experiments were performed as three independent replicates and one-way analysis of variance used for comparison with post hoc Student's *t* tests used to determine statistically significant differences between groups. *P* values less than 0.05 were considered to be statistically significant. HPLC chromatograms and gelatin zymography are representative of three studies.

RESULTS

Mesh Size

Three PEGDA molecular weights were examined at three concentrations (Table I) to fully understand the influence of mesh size on protease entry into the hydrogels. Mesh size is affected by the number of cross-linking groups and the macromer molecular weight (44). Mesh size increases with increased PEGDA macromer molecular weight because there is a larger PEG chain between potential cross-linking points. Mesh size decreases with increased concentration of acrylate groups, as there is a greater number of potential cross-linking groups per volume. The swelling and mesh size measurements followed expected patterns in that larger molecular weight resulted in larger mesh size, and increased concentration decreased mesh size (Fig. 1). Changing the macromer molecular weight had a larger effect on mesh size than changing concentration, but generally both changes had statistically significant effects. There was a statistically significant difference between the 10 and 15 % compositions for all three macromer molecular weights ($p < 0.01$). There was also a statistically significant difference between the 10 and 20 % compositions for PEGDA 3,400 and PEGDA 10,000 ($p < 0.01$). The 15 % (w/v) composition was chosen for release studies as this composition maximized mesh size without compromising hydrogel durability.

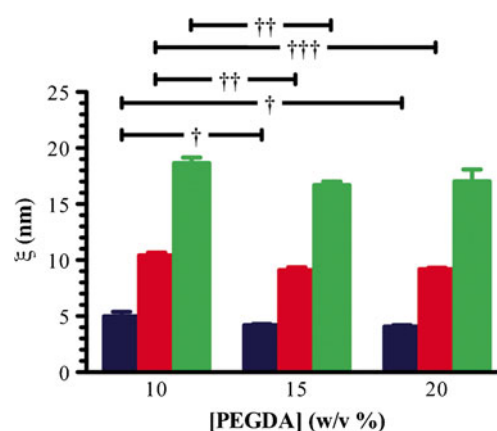


Fig. 1. Mesh size (Greek small letter XI, ξ) measured by swelling. Mesh size increased with increasing PEGDA macromer molecular weight from 3,400 (blue bars) to 10,000 (red bars) and 20,000 (green bars) and with decreased PEGDA macromer content (w/v %) in the precursor solution where all inter-group (molecular weight) differences are significant ($p < 0.001$) and all intra-group differences are marked with †, ††, or ††† indicating $p < 0.05$, $p < 0.01$, and $p < 0.001$, respectively. Values are presented as averages plus or minus (\pm) standard deviation for three independent samples

Release in the Presence of Active MMP-2

It was expected that if MMP-2 was cleaving the peptide and releasing the model drug, there would be greater fluorescence in the buffer when hydrogels were incubated with MMP-2 compared to hydrogels in buffer alone. Hydrogels incubated with MMP-2 without peptide showed little fluorescent signal and no release (Fig. 2a, gray line/symbols) and when no MMP-2 or peptide is present, no release of fluorescence is observed. In all cases where the peptide was present, there was nonspecific release without MMP-2 (dashed lines), and the amount of released peptide increased when MMP-2 was present (solid lines).

From PEGDA 3,400 g/mol hydrogels at 0.15 mM ($p=0.087$) and 1.0 mM ($p=0.105$) peptide loading concentrations, peptide release in the presence of MMP-2 was not significantly different from when no MMP-2 was present (Fig. 2a, c). Interestingly, PEGDA 3,400 g/mol hydrogels released significantly more peptide at the 0.5 mM concentration in the presence of MMP-2 (Fig. 2b; $p=0.005$). All hydrogels formed with all concentrations of PEGDA 10,000 and PEGDA 20,000 showed a significant increase with MMP-2 compared to buffer (Fig. 2d-i) ($0.0001 < p < 0.032$). Actual peptide loading varied among the hydrogels even at identical

concentrations for two reasons. Based upon the reactions between the cysteines and acrylate groups (41), there are fewer acrylate groups available for peptide conjugation as PEGDA molecular weight increases, thus although the peptide amount and total polymer was constant, the ratio of peptide to acrylate groups decreased with molecular weight. Also, the larger molecular weights have a greater amount of swelling further diluting peptide within the hydrogel in the final swollen state. If examined as percent released, there was no significant difference between the loading for a given molecular weight (Fig. 3a). There was also no significant difference in the nonspecific release among the molecular weights at each concentration. In examining the percent released for the different concentrations at each molecular weight, no significant difference was found in the MMP-2 mediated release or the nonspecific release.

However, when the ratio of release with MMP-2 to buffer only at the final time point was calculated (p_r), significant differences were found in comparisons among the molecular weights at the same peptide concentration (Fig. 3b) ($p > 0.05$). While p_r was roughly 2 for all three concentrations of PEGDA 3,400 hydrogels, p_r ranged from 4 to 6 for PEGDA 10,000 and PEGDA 20,000 (Fig. 3b). There was a significant difference in p_r between PEGDA 3,400 and

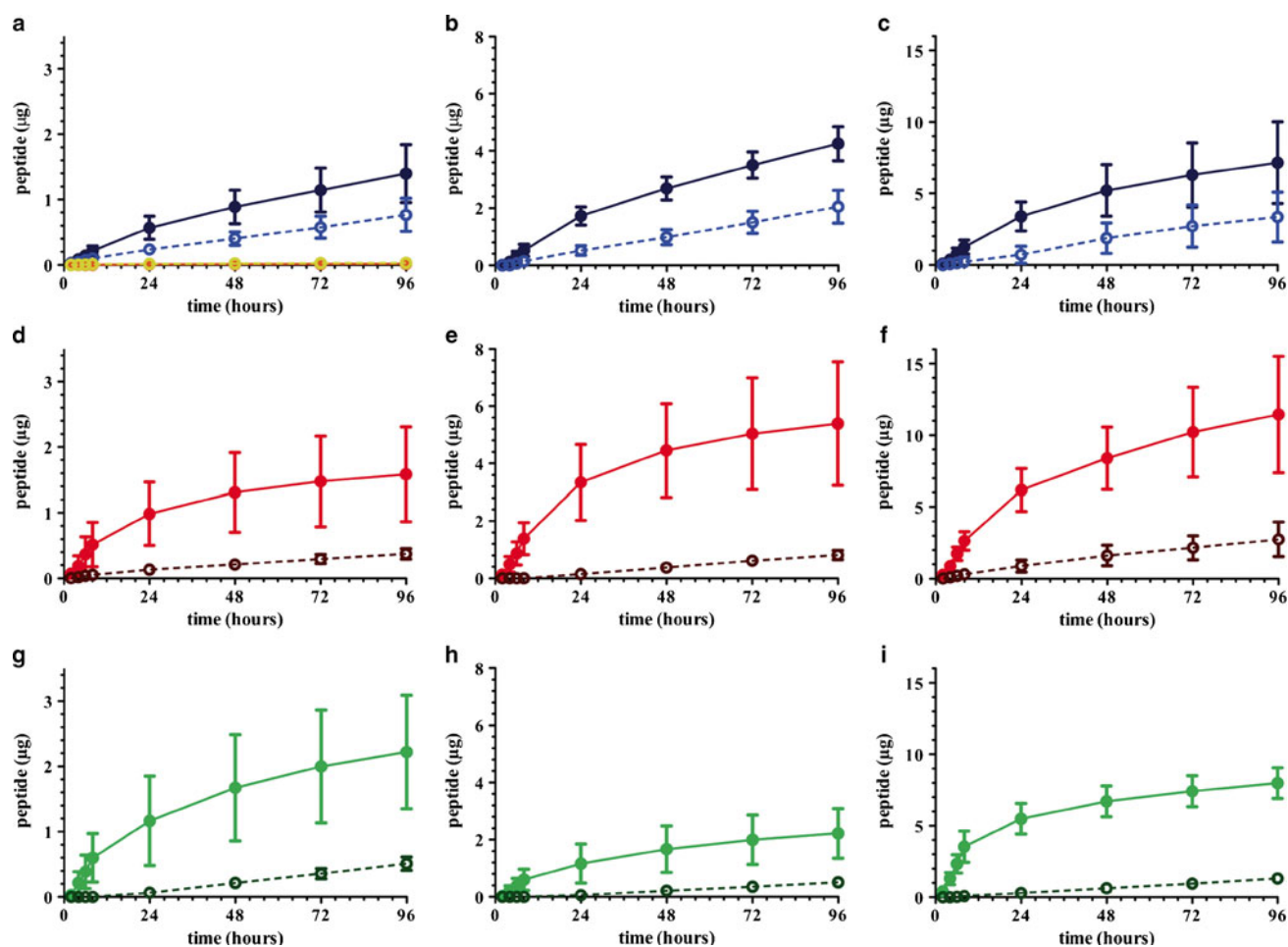


Fig. 2. Peptide release from hydrogels in the presence (filled circle/solid lines) and absence (open circles/dashed lines) active MMP-2. Hydrogels were synthesized from PEGDA MW 3,400 (a-c), 10,000 (d-f), and 20,000 g/mol (g-i); and at peptide loading concentration of 0.15 (a, d, g); 0.5 (b, e, h); 1.0 (c); or 1.75 (f, i) in millimolars. As controls, peptide release when no peptide was included in the hydrogel with and without MMP was plotted (orange and yellow lines) (a). Values are presented as averages plus or minus (\pm) standard deviation for three independent samples

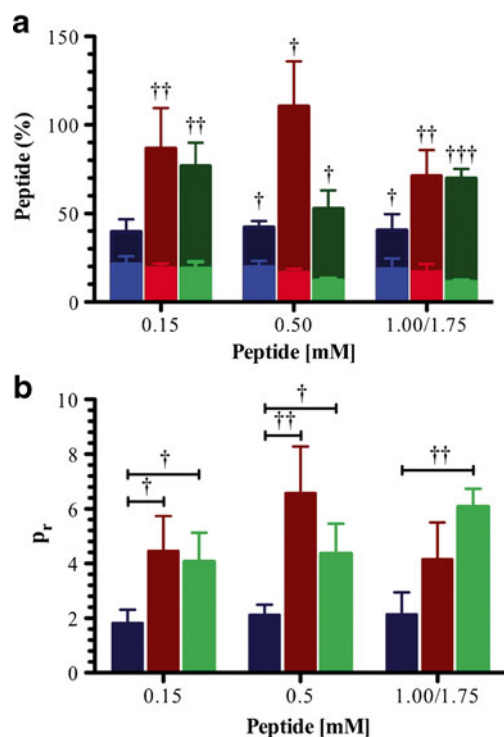


Fig. 3. (a) Peptide release at 96 h (4 days). Percent peptide released from hydrogels at (*x*-axis) 0.15-, 0.5-, and 1.0/1.75-mM peptide concentration following 96 h of incubation in buffer (*light/foreground bar*) or MMP-2 (*dark/background bar*) formulated. Hydrogels were produced at PEGDA molecular weights of (*blue*) 3,400 g/mol, (*red*) 10,000 g/mol, and (*green*) 20,000 g/mol. Values are presented as averages plus or minus (\pm) standard error of the mean for three independent samples and statistical differences between buffer and MMP-2 groups are marked with \dagger , $\dagger\dagger$, or $\dagger\dagger\dagger$ indicating $p < 0.05$, $p < 0.01$, and $p < 0.001$, respectively. Relative peptide release (b). Ratio of peptide released in the presence of MMP-2 to the peptide released in buffer alone (p_r) from 15 % (w/v) PEGDA 3,400 (*blue bars*), PEGDA 10,000 (*red bars*), and PEGDA 20,000 (*green bars*) hydrogels. Values are presented as averages plus or minus (\pm) standard deviation for three independent samples and statistical differences are marked with \dagger and $\dagger\dagger$ indicating $p < 0.05$ and $p < 0.01$, respectively

PEGDA 20,000 at all three concentrations. There was also a significant difference between PEGDA 3,400 and PEGDA 10,000 at the 0.15 and 0.5 mM concentrations ($p < 0.05$). There were no significant differences between PEGDA 10,000 and PEGDA 20,000 at any concentration ($p > 0.05$).

Release in the Presence of U-87 MG Cells

Hydrogels were incubated with U-87 MG cells embedded in collagen to determine if MMP-2 secreted from glioblastoma cells could cleave the MMP-2 sensitive peptide. U-87 MG cells have been shown to activate MMP-2 when in contact with collagen I (45) and this was confirmed in this study (Fig. 4). Similarly, human umbilical cord vascular endothelial cells also express significant active MMP-2 in collagen gels (46) and multiple breast cancer cell lines grown in collagen I gels had significant activation of MMP-2, but those grown on Matrigel, plastic, or thin layers of collagen showed very little activation (47). Even with this released active MMP, it is possible that the MMP does not reach the

hydrogels, enter the hydrogels, or retain activity within the hydrogels.

HPLC fluorescence chromatograms of the supernatant were compared to a chromatogram of the full peptide. Since the cleaved peptide fragment has less hydrophobic surface area than the uncleaved peptide, the cleaved fragment was expected to, and did, elute at an earlier time than the uncleaved peptide. The elution time for the full peptide, TAMRA-GPLGVRGC, was about 15 min (data not shown), while in the presence of cells, a peak was eluted at about 2.5 min for the expected cleaved fragment. This peak was higher in intensity at 24 h than at 8 h and a second peak (or two overlapping peaks) at approximately 4 min was also observed indicating a possible second cleavage site. The sample with hydrogel and without cells had a very small peak at any elution time (Fig. 5). Somewhat surprisingly, a peak was also present in the sample with cells and GM6001 that matched in elution time to the expected cleavage peak by MMP-2 but no 4-min peak was observed.

MALDI-TOF mass spectrometry (MS) was used to analyze the peaks with cells and cells with GM6001 at the 2.5- and 4-min mark from the 24-h time point (Fig. 6). The fractionated peak at 2.5-min elution time with cells demonstrates a compound at 754.84 mass charge ratio (m/z). This molecular weight corresponds to TAMRA-GPLG, the anticipated cleavage fragment from MMP-2. The 4-min peak had one predominant species with a 1,010 mass charge ratio (m/z) corresponding to TAMRA-GPLGVR (Fig. 6). No peak was present at this mass in the sample with cells and GM6001, but a new peak at 574.87 was the predominant peak corresponding to the TAMRA-GP fragment. In each, TAMRA was also observed. This suggested that there was alternate protease acting within the hydrogels. In the absence of cells, the predominant peak from HPLC and MALDI-TOF MS was the intact peptide (data not shown).

Gelatin zymography of conditioned media from U-87 MG cells embedded in collagen identified the presence of active MMP-2 (Fig. 4). An unidentified band was present in the gel at a lower molecular weight than MMP-2. This gelatinolytic enzyme may also be contributing to cleavage of the MMP-2 sensitive peptide and model drug release, but it appears that when MMP-2 is present, the predominant cleavage is by MMP-2 with limited TAMRA-GP peptide observed from the alternate cleavage/protease.

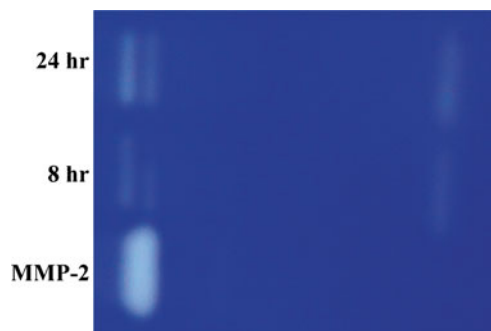


Fig. 4. MMP-2 and at least one other gelatinolytic peptide are produced by U-87 MG cells. Gelatin zymography of supernatant collected from U-87 MG cells seeded in collagen gels at 8 and 24 h and 9 nM MMP-2

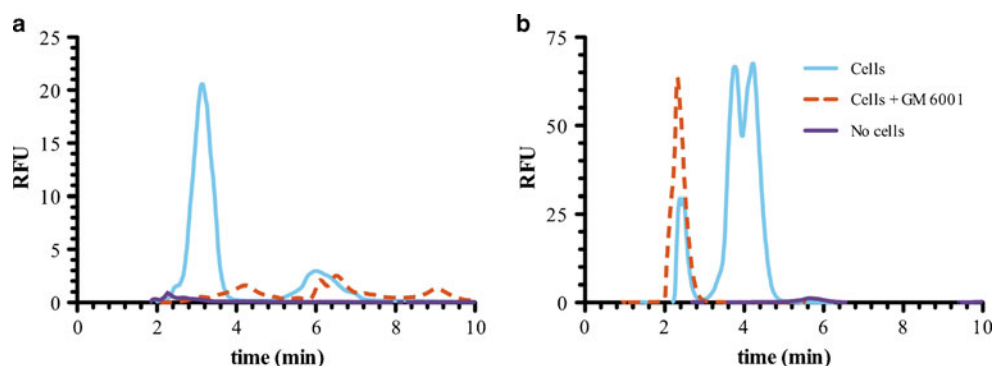


Fig. 5. Representative HPLC fluorescence chromatograms of supernatant media from U-87 MG incubated with hydrogels in the absence (*purple*), in the presence of cells (*light blue*), and in the presence of cells incubated with GM6011 (*orange*) for (a) 8 h and (b) 24 h

DISCUSSION

The hydrogel mesh affects the ability of MMP-2 to enter the hydrogel; a mesh smaller than MMP-2 dimensions will prohibit entry (48). Mesh differs from pores in that a pore is a space in which polymer is continuously absent. Mesh describes the space bordered by polymer chains and cross-links at a given instant of time, but that space may be occupied by polymer in the next instant due to thermal fluctuation of the polymer chains. The hydrogels used in this application were nonporous; MMP-2 entry and diffusion of cleaved products was primarily influenced by the mesh.

The MMP-2 molecule is a prolate ellipsoid with dimensions of approximately 9.75 nm in length and 6.75 nm in breadth (49). PEGDA 20,000 and the PEGDA 10,000 hydrogels produced in this study had a mesh size larger than both of the two axes of MMP-2 at a 15 % w/V composition (16.71 ± 0.30 and 9.11 ± 0.25 , respectively). The PEGDA 3,400 hydrogels mesh size for this composition was 4.19 ± 0.01 , smaller than either axis of MMP-2. Therefore, PEGDA 3,400 was expected to have a limited release compared to PEGDA 10,000 and PEGDA 20,000. These results are in agreement with our prior results that showed a minimum of PEGDA 4,000 was necessary for MMP-based release (5) and PEGDA 4,000 and 8,000 hydrogels had no more than 80 % release.

Significant differences were not seen between the 15 and 20 % for PEGDA 10,000 and PEGDA 20,000. A potential reason is that as the hydrogel polymerizes, the polymer solution becomes more viscous. Although there may be additional acrylate groups, they cannot form additional cross-links due to the inability to physically move through the solution, a phenomenon seen in chain growth polymerizations known as the gel effect (50,51). It is also possible that the differences between the mesh sizes are not sufficient for detection. Beyond changes in the mesh size of the hydrogel due to pendant unreacted acrylate groups, these unreacted groups may influence toxicity of the hydrogels and react with diffusing proteins and other biomolecules. As it was not the focus of this project, we did not assess the extent of pendant acrylates. Using a similar system, Salinas and Anseth proposed a model for peptide incorporation and correlated thiol conversion to acrylate conversion (41). Using rough approximation based upon our thiol conversion, we had on the order of 85 % conversion of acrylate groups in the system.

There are also several limitations to the calculations of molecular weight between cross-links and mesh sizes. One pertinent factor in the measurement is that these measurements were made without the incorporation of the MMP cleavable peptide, GPLGVRGC. Peptide conjugation to PEGDA reduces acrylate groups available for cross-linking opening the mesh of the network. The presence of arginine in the MMP cleavable sequence and carboxyl groups on TAMRA resulted in a zwitterionic hydrogel at physiological pH, a condition for which an equation for molecular weight between cross-links has not been developed. The concentration of peptide groups is low enough compared to acrylate group concentration; therefore, the measurements without peptide are a close approximation to mesh size with incorporated peptide. Irregularities within the hydrogel structure may further limit the accuracy of the mesh size measurement. The equation for molecular weight between cross-links assumes all polymer chains are perfectly cross-linked. In practice, hydrogels have noncross-linked (pendant) polymer chains throughout the matrix. However, the models accurately predict the increase in specific release as the hydrogel mesh size increases.

An estimated diffusion coefficient through the hydrogels was calculated based upon the analysis conducted by Peppas and Lustig (48). The unhindered diffusion coefficient, D_0 , was calculated using the Stokes–Einstein equation. The MMP-2 molecule was modeled as a prolate ellipse and hydrodynamic

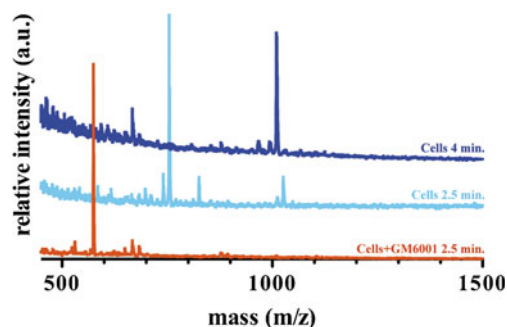


Fig. 6. Representative MALDI-TOF mass spectra of peptide fractions collected from the 2.5- and 4-min peaks of HPLC chromatography (Fig. 5b) of peptides release from hydrogels in the presence of cells (*Cells*) and in the presence of cells incubated with GM6001 (*Cells+GM6001*)

Table II. Properties Calculated for MMP-2 Diffusion Through Hydrogels at 15 (w/V) % PEGDA

PEGDA molecular weight (g/mol)	Mesh size (nm) ^a	D_e (cm ² /s) ^b	L (cm) ^c	τ (h) ^d
3,400	4.19	N/A	0.075	N/A
10,000	9.11	3.13×10^{-7}	0.09	7.19
20,000	16.71	4.77×10^{-7}	0.1	5.82

^a Calculated using Flory–Rehner theory as adapted by Peppas *et al.* for polymerization in the presence of solvent (57)

^b Calculated using Stokes–Einstein equation corrected for a prolate ellipsoid (58) of approximate size of MMP-2

^c Measured using a digital caliper

^d Tanaka time scaling factor for swelling of a hydrogel (53)

radius calculation used for molecule radius (52). Diffusion time scaling factor, τ , through the hydrogel was calculated according to Tanaka (53). The scaling factor, as an estimate of time that it would take for a molecule to reach the center of the hydrogel, was calculated for all three hydrogels at 15 % w/V (Table II). The validity of this calculation is limited by several factors including the structural inhomogeneities implicit in the hydrogel production and the ionic nature of the hydrogel. MMP-2 orientation in relation to the mesh will vary and consequently affect diffusion. The contributions to release from surface peptide cleavage also contribute to the release of MMP-2. It is clear from this analysis that there is limited MMP-specific release expected for lower molecular weight PEGDA-based hydrogels, while the higher molecular weight allowed more significant release.

But, purified MMP is not the only factor influencing release from the hydrogels as cellular proteases are tightly regulated. U-87 MG cells released cleaved peptide fragments as clearly observed by the reduced elution time. We did not use fluorescence to quantify release due to limitations reproducibly recovering peptide fragments from the collagen gels. When cells were incubated with GM6001, there was also release to a lesser extent, and the identity appeared equivalent by HPLC. However, the MS analysis of both peaks shows the absence of TAMRA-GPLG peak, indicating the inhibition of MMP-2 cleavage as this was the primary peak in the presence of MMP-2. The peak observed with HPLC of cell supernatants obtained in the presence of GM6001 is likely due to other proteases expressed by the cells. Since GM6001 is a broad spectrum MMP inhibitor, it is unlikely other MMPs are responsible for this cleavage, but not impossible. Gelatin zymography confirmed the expression and activation by MMP-2 by U-87 MG cells. Gelatin zymography suggests that there is a low molecular weight gelatinolytic protease present. MMP-1, MMP-8, and MMP-13 can be visible in gelatin zymography, but band intensity is typically much less compared to MMP-2 and no peaks are present in the appropriate regions of the zymogram (54). Inclusion of these and other proteases in zymography may elucidate the identity of this low molecular weight gelatinolytic protease. MMP-7 is a relatively low molecular weight metalloproteinase with gelatinolytic properties and has been known to be expressed by brain tumors (55,56). There are many proteases that could explain this new cleavage peak and the observed protease may or may not be related to the observed cleavage peak. We plan to further investigate this in the future, but the result clearly shows that the release of peptide conjugates is modulated by MMP inhibition and multiple proteases can be used for selective release in a

fashion similar to the normal release from the extracellular matrix of biologically active peptides.

CONCLUSION

The mesh size and release data support the fact that MMP-2 enters into PEGDA hydrogels of sufficient mesh size. There is clearly greater specific release, as described by the ratio of release in the presence to the absence of MMP-2, at PEGDA macromer molecular weights that have a large enough mesh size. An optimal PEGDA composition was determined to be 15 % w/V where 100 % of peptide is released in response to MMP. PEGDA 10,000 or PEGDA 20,000 was equally well suited for optimal macromer molecular weight, as no significant difference was seen between the groups. The release was confirmed in the presence of MMP-2, but also in the presence of cells growing in three-dimensional culture. Interestingly, when cells are grown in three-dimensional culture and inhibited with a general MMP inhibitor, a new peptide fragment is released and a small gelatinolytic peptide can be identified. This suggests that the redundant nature of proteases can be used to activate release from this system in response to multiple proteases.

ACKNOWLEDGMENT

The authors would like to thank Dr. William Beck for use of equipment. We thank Dr. J.H. “Robert” Chang for insightful discussion. This work was supported by NIH R01 NS055095 (RAG). This investigation was conducted in a facility constructed with support from Research Facilities Improvement Program Grant Number C06 RR15482 from the National Center for Research Resources, NIH.

REFERENCES

1. Central Brain Tumor Registry of the United States. Statistical report: primary brain tumors in the United States, 1992–1997, 2001. 2001.
2. Siegel R, Ward E, Brawley O, Jemal A. Cancer statistics, 2011. *CA Cancer J Clin.* 2011;61(4):212–36.
3. Wen PY, Kesari S. Malignant gliomas in adults. *N Engl J Med.* 2008;359(5):492–507.
4. Central Brain Tumor Registry of the United States. Primary Brain Tumors in the United States. Chicago, IL. 2007–2008.
5. Tauro JR, Gemeinhart RA. Extracellular protease activation of chemotherapeutics from hydrogel matrices: a new paradigm for local chemotherapy. *Mol Pharm.* 2005;2(5):435–8.
6. Tauro JR, Gemeinhart RA. Matrix metalloproteinase triggered local delivery of cancer chemotherapeutics. *Bioconjug Chem.* 2005;16(5):1133–9.

7. Tauro JR, Lee BS, Lateef SS, Gemeinhart RA. Matrix metalloprotease selective peptide substrates cleavage within hydrogel matrices for cancer chemotherapy activation. *Peptides*. 2008;29(11):1965–73.
8. Anseth KS, Bowman CN, Brannon-Peppas L. Mechanical properties of hydrogels and their experimental determination. *Biomaterials*. 1996;17(17):1647–57.
9. Peppas NA, Bures P, Leobandung W, Ichikawa H. Hydrogels in pharmaceutical formulations. *Eur J Pharm Biopharm*. 2000;50(1):27–46.
10. Kim SW, Bae YH, Okano T. Hydrogels: swelling, drug loading, and release. *Pharm Res*. 1992;9(3):283–90.
11. Levi E, Fridman R, Miao HQ, Ma YS, Yayon A, Vlodavsky I. Matrix metalloproteinase 2 releases active soluble ectodomain of fibroblast growth factor receptor 1. *Proc Natl Acad Sci USA*. 1996;93(14):7069–74.
12. Overall CM, Kleifeld O. Validating matrix metalloproteinases as drug targets and anti-targets for cancer therapy. *Nat Rev Cancer*. 2006;6(3):227–39.
13. Overall CM, Lopez-Otin C. Strategies for MMP inhibition in cancer: innovations for the post-trial era. *Nat Rev Cancer*. 2002;2(9):657–72.
14. Vartak D, Gemeinhart RA. Matrix metalloproteases: underutilized targets for drug delivery. *J Drug Target*. 2007;15(1):1–21.
15. Fridman R. Surface association of secreted matrix metalloproteinases. *Cell Surf Proteases*. 2003;54:75–100.
16. Foda HD, Zucker S. Matrix metalloproteinases in cancer invasion, metastasis and angiogenesis. *Drug Discov Today*. 2001;6(9):478–82.
17. Haas TL, Madri JA. Extracellular matrix-driven matrix metalloproteinase production in endothelial cells: implications for angiogenesis. *Trends Cardiovasc Med*. 1999;9(3–4):70–7.
18. Lu MK, Chen PH, Shih YW, Chang YT, Huang ET, Liu CR, *et al.* alpha-Chaconine inhibits angiogenesis *in vitro* by reducing matrix metalloproteinase-2. *Biol Pharm Bull*. 2010;33(4):622–30.
19. Rao JS, Yamamoto M, Mohaman S, Gokaslan ZL, Fuller GN, Stetler-Stevenson WG, *et al.* Expression and localization of 92 kDa type IV collagenase/gelatinase B (MMP-9) in human gliomas. *Clin Exp Metastasis*. 1996;14(1):12–8.
20. Sawaya RE, Yamamoto M, Gokaslan ZL, Wang SW, Mohanam S, Fuller GN, *et al.* Expression and localization of 72 kDa type IV collagenase (MMP-2) in human malignant gliomas *in vivo*. *Clin Exp Metastasis*. 1996;14(1):35–42.
21. Chau Y, Tan FE, Langer R. Synthesis and characterization of dextran-peptide-methotrexate conjugates for tumor targeting via mediation by matrix metalloproteinase II and matrix metalloproteinase IX. *Bioconjug Chem*. 2004;15(4):931–41.
22. Chau Y, Langer RS. Important factors in designing targeted delivery of cancer therapeutics via MMP-2 mediation. *J Control Release*. 2003;91(1–2):239–40.
23. Albright CF, Graciani N, Han W, Yue E, Stein R, Lai ZH, *et al.* Matrix metalloproteinase-activated doxorubicin prodrugs inhibit HT1080 xenograft growth doxorubicin with less toxicity. *Mol Cancer Ther*. 2005;4(5):751–60.
24. Lim SH, Jeong YI, Moon KS, Ryu HH, Jin YH, Jin SG, *et al.* Anticancer activity of PEGylated matrix metalloproteinase cleavable peptide-conjugated adriamycin against malignant glioma cells. *Int J Pharm*. 2010;387(1–2):209–14.
25. Bae M, Cho S, Song J, Lee GY, Kim K, Yang J, *et al.* Metalloprotease-specific poly(ethylene glycol) methyl ether-peptide-doxorubicin conjugate for targeting anticancer drug delivery based on angiogenesis. *Drugs Exptl Clin Res*. 2003;29(1):15–23.
26. Lee GY, Park K, Kim SY, Byun Y. MMPs-specific PEGylated peptide-DOX conjugate micelles that can contain free doxorubicin. *Eur J Pharm Biopharm*. 2007;67(3):646–54.
27. Terada T, Iwai M, Kawakami S, Yamashita F, Hashida M. Novel PEG-matrix metalloproteinase-2 cleavable peptide-lipid containing galactosylated liposomes for hepatocellular carcinoma-selective targeting. *J Control Release*. 2006;111(3):333–42.
28. Tokatljan T, Shrum CT, Kadoya WM, Segura T. Protease degradable tethers for controlled and cell-mediated release of nanoparticles in 2- and 3-dimensions. *Biomaterials*. 2010;31(31):8072–80.
29. Laromaine A, Koh LL, Murugesan M, Ulijn RV, Stevens MM. Protease-triggered dispersion of nanoparticle assemblies. *J Am Chem Soc*. 2007;129(14):4156–7.
30. Rawsterne RE, Gough JE, Rutten FJM, Pham NT, Poon WCK, Flitsch SL, *et al.* Controlling protein retention on enzyme-responsive surfaces. *Surf Interface Anal*. 2006;38(11):1505–11.
31. Thornton PD, McConnell G, Ulijn RV. Enzyme responsive polymer hydrogel beads. *Chem Commun*. 2005;47:5913–5.
32. Ulijn RV. Enzyme-responsive materials: a new class of smart biomaterials. *J Mater Chem*. 2006;16(23):2217–25.
33. West JL, Hubbell JA. Polymeric biomaterials with degradation sites for proteases involved in cell migration. *Macromolecules*. 1999;32(1):241–4.
34. Lutolf MP, Hubbell JA. Synthetic biomaterials as instructive extracellular microenvironments for morphogenesis in tissue engineering. *Nat Biotechnol*. 2005;23(1):47–55.
35. Lutolf MP, Lauer-Fields JL, Schmoekel HG, Metters AT, Weber FE, Fields GB, *et al.* Synthetic matrix metalloproteinase-sensitive hydrogels for the conduction of tissue regeneration: engineering cell-invasion characteristics. *Proc Natl Acad Sci USA*. 2003;100(9):5413–8.
36. Zisch AH, Lutolf MP, Ehrbar M, Raeber GP, Rizzi SC, Davies N, *et al.* Cell-demanded release of VEGF from synthetic, biointeractive cell ingrowth matrices for vascularized tissue growth. *FASEB J*. 2003;17(15):2260–2.
37. Gojgini S, Tokatljan T, Segura T. Utilizing cell-matrix interactions to modulate gene transfer to stem cells inside hyaluronic acid hydrogels. *Mol Pharm*. 2011;8(5):1582–91.
38. Peppas NA, Keys KB, Torres-Lugo M, Lowman AM. Poly(ethylene glycol)-containing hydrogels in drug delivery. *J Control Release*. 1999;62(1–2):81–7.
39. Kim J, Hefferan TE, Yaszemski MJ, Lu L. Potential of hydrogels based on poly(ethylene glycol) and sebacic acid as orthopedic tissue engineering scaffolds. *Tissue Eng, Part A*. 2009;15(8):2299–307.
40. Bryant SJ, Lynn AD, Kyriakides TR. Characterization of the *in vitro* macrophage response and *in vivo* host response to poly(ethylene glycol)-based hydrogels. *J Biomed Mater Res A*. 2010;93A(3):941–53.
41. Salinas CN, Anseth KS. Mixed mode thiol-acrylate photopolymerizations for the synthesis of PEG-peptide hydrogels. *Macromolecules*. 2008;41(16):6019–26.
42. Hughes SW. Archimedes revisited: a faster, better, cheaper method of accurately measuring the volume of small objects. *Phys Educ*. 2005;40(5):468–74.
43. Peppas NA. *Hydrogels in medicine and pharmacy*. Boca Raton: CRC Press; 1986.
44. Flory PJ. *Principles of polymer chemistry*. Ithaca: Cornell University Press; 1953.
45. Vartak DG. Integrins and matrix metalloprotease-2 as dual targets in angiogenesis. Ph.D. Dissertation, University of Illinois at Chicago, Chicago; 2009.
46. Vartak DG, Gemeinhart RA. *In vitro* evaluation of functional interaction of integrin $\alpha v \beta 3$ and matrix metalloprotease-2. *Mol Pharm*. 2009;6(6):1856–67.
47. Azzam HS, Arand G, Lippman ME, Thompson EW. Association of MMP-2 activation potential with metastatic progression in human breast cancer cell lines independent of MMP-2 production. *J Natl Cancer Inst*. 1993;85(21):1758–64.
48. Lustig S, Peppas NA. Solute diffusion in swollen membranes. IX. Scaling laws for solute diffusion in gels. *J Appl Polym Sci*. 1988;36(4):735–47.
49. Morgunova E, Tuuttilla A, Bergmann U, Isupov M, Lindqvist Y, Schneider G, *et al.* Structure of human pro-matrix metalloproteinase-2: activation mechanism revealed. *Science*. 1999;284(5420):1667–70.
50. Cowie JMG, Arrighi V. *Polymers: chemistry and physics of modern materials*. 3rd ed. Boca Raton: CRC Press; 2008.

51. Brannon-Peppas L. Preparation and characterization of cross-linked hydrophilic networks. In: Brannon-Peppas L, Harland RS, editors. *Absorbent Polymer Technology*. Amsterdam: Elsevier; 1990. p. 45–65.
52. Hansen S. Translational friction coefficients for cylinders of arbitrary axial ratios estimated by Monte Carlo simulation. *J Chem Phys*. 2004;121(18):9111–5.
53. Tanaka T, Fillmore DJ. Kinetics of swelling gels. *J Chem Phys*. 1970;70(3):1214–8.
54. Snoek-van Beurden PAM, Von den Hoff JW. Zymographic techniques for the analysis of matrix metalloproteinases and their inhibitors. *Biotechniques*. 2005;38(1):73–83.
55. Rome C, Arsaut J, Taris C, Couillaud F, Loiseau H. MMP-7 (matrilysin) expression in human brain tumors. *Mol Carcinog*. 2007;46(6):446–52.
56. Woessner Jr JF, Taplin CJ. Purification and properties of a small latent matrix metalloproteinase of the rat uterus. *J Biol Chem*. 1988;263(32):16918–25.
57. Peppas NA, Huang Y, Torres-Lugo M, Ward JH, Zhang J. Physicochemical, foundations and structural design of hydrogels in medicine and biology. *Annu Rev Biomed Eng*. 2000;2:9–29.
58. Cussler EL. *Diffusion: mass transfer in fluid systems*. 3rd ed. Cambridge: Cambridge University Press; 2009.